Journal of Chemical&Engineering Data

pubs.acs.org/jced Article

Liquid-Phase Speed of Sound and Vapor-Phase Density of Difluoromethane

Aaron J. Rowane,* Elizabeth G. Rasmussen, and Mark O. McLinden

Cite This: https://doi.org/10.1021/acs.jced.2c00441 Read Online

ACCESS | Metrics & More | Article Recommendations | Supporting Information

ABSTRACT: Difluoromethane (HFC-32, DFM), with a global warming potential (GWP) of 677, is of interest as a pure refrigerant and as a component in low-GWP refrigerant mixtures. Additionally, difluoromethane has recently been identified as a safe, liquefied-gas electrolyte material in batteries. Using state-of-the-art instruments for measurements, this paper presents new liquid-phase speed of sound and vapor-phase density data for difluoromethane. Two hundred and nine liquid-phase speed of sound values were measured using a dual-path pulse-echo instrument at temperatures from 230 to 345 K and pressures from 2.1 to 70 MPa. Accounting for all sources of uncertainty, the relative expanded combined uncertainty ($k = 2$) in the speed of sound ranged from 0.035 to 0.17%. One hundred and thirty-eight vapor-phase density values were measured using a two-sinker densimeter at temperatures from 240 to 340 K and pressures from 0.1 to 1.61 MPa with an uncertainty of 0.011 to 0.12%. These experimental data will be valuable in the ongoing development of a new fundamental thermodynamic equation of state for difluoromethane.

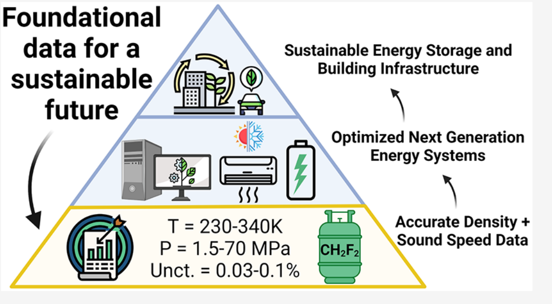

1. INTRODUCTION

Growing industrial activities in emerging economies have significantly increased demand for refrigerants, with the global refrigerant market size forecasted to reach USD 27.2 billion by 2025.[1] Refrigeration provides large societal benefits, but it also accounts for 7.8% of global greenhouse gas emissions.[2] Switching from refrigerant fluids currently in use to low-global warming potential (GWP) refrigerant fluids could avert nearly 3% of global greenhouse emissions, with larger impacts as the demand for refrigerants grows.[3]

Difluoromethane (CAS 75-10-5), also known as HFC-32 or DFM, with the chemical formula CH_2F_2 and a molar mass of 52.024 g mol^{-1}, has a 100-year GWP of 677.[4] Difluoromethane is a component of the widely used refrigerant R-410A (which is a blend of 50 mass % difluoromethane and 50 mass % pentafluoroethane). It is also increasingly used as a pure-fluid refrigerant. In 2015, difluoromethane was approved for use in self-contained room air conditioners under the United States Environmental Protection Agency's Significant New Alternatives Program;[5] this approval was expanded in 2021 to additional types of residential and light-commercial air-conditioning systems and heat pumps.[6] Furthermore, difluoromethane is a component in numerous low-GWP refrigerant blends; it appears in a total of 56 refrigerant blends classified in ASHRAE Standard 34,[7] including a majority of the low- and moderate-GWP blends introduced in the last 5 years. In addition to its use in the refrigeration industry, difluoromethane is actively being investigated by the energy storage industry as a liquified-gas electrolyte material in batteries.[8−10]

An equation of state (EOS) is a mathematical relation between thermodynamic state variables. In simulations seeking to optimize next-generation sustainable technologies, like refrigeration cycles or batteries, EOS guides results on a material's thermodynamic behavior in the system. While there are several EOS in the literature,[11,12] the Helmholtz-energy-explicit fundamental EOS by Tillner-Roth and Yokozeki[13] is the most robust; it forms the basis for the ISO standard on refrigerant properties,[3] and it is the EOS implemented in the National Institute of Standards and Technology (NIST) REFPROP database.[14] In fitting mixture data for other low-GWP refrigerant blends recently measured in our group,[5,15,16] Bell[17] concluded that the inability to fit speed of sound data for the R-134a/1234ze(E) blend to within its experimental uncertainty was likely due to deficiencies in the pure-fluid EOS for R-1234ze(E) (*trans*-1,3,3,3-tetrafluoropropene).[18] As our group had also recently measured blends containing HFC-32,[16,18] this led us to examine the EOS for difluoromethane.

Tillner-Roth and Yokozeki do not provide an estimated uncertainty for speed of sound calculated with their EOS, but they estimated an uncertainty of 0.5−1.0% for the related thermodynamic quantity of isobaric heat capacity. This is

Received: July 8, 2022
Accepted: September 6, 2022

much higher than the uncertainties realized by state-of-the-art speed of sound instruments. This motivated the efforts reported in this paper to measure the liquid-phase speed of sound for difluoromethane. Additionally, an examination of the NIST Thermodynamics Research Center tool ThermoPlan indicated that limited liquid-phase speed of sound and vapor-phase density data of difluoromethane are reported in the literature.[19−22] Thus, vapor-phase density measurements were also completed and are presented in this paper. Figure 1 shows the range of conditions investigated in this paper (solid green circles) and by previous literature studies.

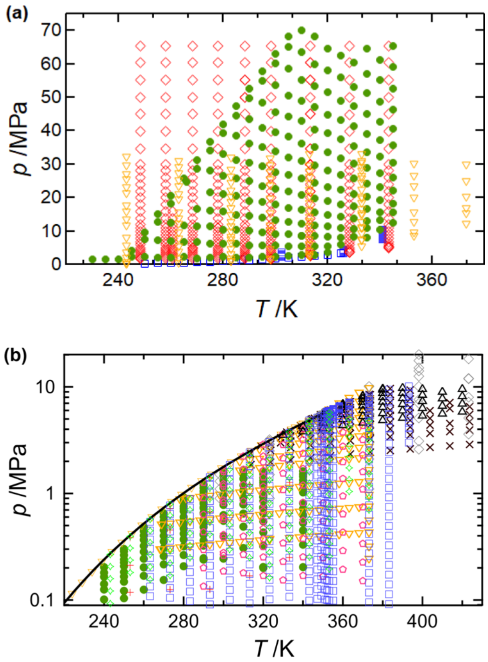

Figure 1. Experimental points measured for difluoromethane; (a) liquid-phase speed of sound: green circle solid, this work; red diamond open, Pires and Guedes;[23] blue box, Grebenkov et al.;[24] and orange triangle down open, Takagi.[25] (b) Vapor-phase density: green circle solid, this work; red plus, Bouchot and Richon;[26] blue box, de Vries;[27] ×, Fukushima et al.; green four headed star, Fu et al.;[28] orange triangle down open, Defibaugh et al.;[29] triangle up open, Sato et al.;[30] pink pentagon, Qian et al.;[31] and diamond open, Malbrunot et al.;[32] the solid line is the saturation boundary.

In turn, this paper presents new data on the liquid-phase speed of sound and vapor-phase density of difluoromethane. A dual-path pulse-echo instrument was used to measure the liquid-phase speed of sound at temperatures from 230 to 345 K, with pressures from 2.1 to 70 MPa. A two-sinker densimeter was used to measure vapor-phase densities at temperatures from 240 to 340 K and pressures from 0.1 to 1.61 MPa. An uncertainty analysis and comparisons of the measured data to the Tillner-Roth and Yokozeki EOS are presented. By using state-of-the-art instrumentation to characterize difluoromethane, the data presented here can be valuable in efforts to develop an improved Helmholtz-energy-explicit EOS for this fluid.

2. MATERIALS AND METHODS

2.1. Experimental Samples. The materials used in this study are outlined in Table 1 along with their molecular formula, molar mass, source, and purity. Purities were reported by the supplier and confirmed by our own tests with gas chromatography/mass spectrometry (GC−MS). Samples were loaded into cleaned and evacuated type 316L stainless-steel sample cylinders; volatile impurities (e.g., air) were removed by the freeze/pump/thaw method as previously described.[16]

2.2. Dual-Path Pulse-Echo Instrument. The dual-path pulse-echo instrument used to measure the speed of sound has been described in detail elsewhere, and only key details are outlined here.[33−35] At the heart of the instrument, a quartz crystal, acting as both an ultrasonic signal transmitter and receiver, is immersed in the sample fluid. A 10-cycle sinusoidal tone burst from an arbitrary function generator excites the crystal at its resonance frequency of 8.00 MHz; the generated tone burst thus emitted from both faces of the crystal traverses the fluid along short and long paths of 12 and 30 mm defined by tubular spacers before returning from flat reflectors at each end of the sample volume. The crystal transducer receives the echoes, which it converts to an electrical signal, which then passes through a three-stage amplifier before being recorded using a digital storage oscilloscope. The speed of sound is determined by

$$c = \frac{2(L_{\text{long}} - L_{\text{short}})}{\Delta t} \quad (1)$$

where L_{long} and L_{short} are the lengths of the tubular spacers and Δt is the time delay between the short- and long-path echo times. The term $(L_{\text{long}} - L_{\text{short}})$ is a function of temperature and pressure determined by calibration with propane as previously described in the literature.[33,35] It is important to note that velocity dispersion, when the measured sonic velocity is not equivalent to the thermodynamic speed of sound, has been observed in some measurements. This occurs when the instrument's operating frequency is too high such that the molecule's internal degrees of freedom take too long to achieve thermodynamic equilibrium relative to the frequency of the propagating sound wave. This behavior was observed, for example, by El Hawary et al.[36] for speed of sound measurements of isopentane at an operating frequency of 8 MHz and was characterized by a significant dampening of the echo signals at lower temperatures. Such behavior was not

Table 1. Materials Used in This Study with Their CAS Numbers, Molar Mass, Source, and Purity

chemical name	CAS number	molar mass ($g \cdot mol^{-1}$)	source	purity as supplied (mole fracton)	purification method	final purity (mole fraction)	analytical method
Difluoromethane[a]	75-10-5	52.02	Advanced Specialty Gases	0.9999	freeze/pump/thaw	0.9999	GC/MS
Difluoromethane[b]	75-10-5	52.02	DuPont	0.9999	freeze/pump/thaw	0.9999	GC/MS
propane	74-98-6	44.10	Scott Specialty Gases	0.99999	freeze/pump/thaw	0.99999	GC/MS

[a]Sample used for the speed-of-sound measurements. [b]Sample used for $(p-\rho-T)$ measurements.

Table 2. Experimental Liquid-Phase Speed of Sound Data for Difluoromethane[a,b]

T/K	p/MPa	c/m·s^{-1}	$100 \cdot U_c(c)/c$	T/K	p/MPa	c/m·s^{-1}	$100 \cdot U_c(c)/c$
229.998	1.524	941.54	0.038	284.997	25.686	825.90	0.039
235.010	1.528	915.36	0.038	289.999	30.373	833.59	0.038
240.000	1.561	888.92	0.038	294.992	35.054	841.19	0.038
244.999	2.227	866.49	0.039	299.995	39.645	848.16	0.037
250.000	7.503	873.70	0.039	304.995	44.256	855.20	0.037
254.991	12.824	881.26	0.038	309.998	48.851	862.08	0.036
259.985	20.495	901.78	0.037	314.992	53.408	868.74	0.036
264.994	25.892	909.11	0.037	320.001	57.960	875.28	0.036
269.990	31.285	916.45	0.036	325.007	62.482	881.65	0.035
274.993	36.683	923.75	0.036	264.992	2.295	758.75	0.046
279.998	42.045	930.84	0.035	269.989	6.787	767.32	0.044
284.999	47.349	937.66	0.035	274.992	11.336	776.10	0.043
290.000	52.634	944.35	0.035	279.996	15.898	784.77	0.042
294.996	57.875	950.85	0.035	284.997	20.444	793.19	0.041
299.999	63.096	957.22	0.034	289.999	24.948	801.17	0.040
304.995	68.285	963.48	0.034	294.994	29.434	808.95	0.039
244.999	2.227	866.49	0.039	299.995	33.923	816.60	0.039
250.000	7.503	873.70	0.039	304.994	38.405	824.11	0.038
254.991	12.824	881.26	0.038	309.996	42.860	831.36	0.037
259.984	18.158	888.88	0.037	314.992	47.262	838.28	0.037
266.140	24.652	897.88	0.038	320.000	51.633	844.93	0.037
269.990	28.774	903.63	0.037	325.006	56.010	851.56	0.036
274.992	34.055	910.82	0.036	329.998	60.366	858.06	0.036
279.997	39.343	918.00	0.036	335.002	64.648	864.14	0.036
284.998	44.583	924.94	0.035	269.984	1.857	727.16	0.049
290.000	49.772	931.62	0.035	274.988	6.132	736.07	0.047
294.995	54.919	938.10	0.035	279.994	10.462	745.19	0.045
299.996	60.039	944.44	0.035	284.995	14.791	754.08	0.044
304.994	65.139	950.67	0.035	289.997	19.104	762.64	0.043
309.997	70.054	956.18	0.034	294.993	23.402	770.93	0.041
249.997	2.216	839.73	0.041	299.995	27.679	778.92	0.041
254.989	7.400	848.00	0.040	304.993	31.960	786.76	0.040
259.982	12.589	856.23	0.039	309.996	36.220	794.35	0.039
274.992	28.035	879.59	0.037	314.991	40.454	801.70	0.039
279.999	33.170	887.12	0.037	320.000	44.668	808.80	0.038
284.998	38.414	895.12	0.036	325.007	48.852	815.65	0.038
290.000	43.508	902.36	0.036	329.997	53.002	822.29	0.037
294.995	48.536	909.24	0.036	335.001	57.123	828.69	0.037
299.997	53.535	915.92	0.035	340.006	61.211	834.88	0.036
304.995	58.493	922.39	0.035	345.011	65.282	840.95	0.036
309.998	63.420	928.70	0.035	274.989	2.089	700.78	0.052
314.992	68.306	934.83	0.035	279.995	6.228	710.45	0.049
254.988	2.133	812.19	0.042	284.996	10.375	719.88	0.047
259.982	6.973	819.87	0.041	289.999	14.525	729.04	0.046
264.989	11.650	826.39	0.040	294.994	18.643	737.74	0.044
269.986	16.541	834.32	0.039	299.995	22.767	746.23	0.043
274.991	21.629	843.25	0.039	304.995	26.869	754.39	0.042
279.995	26.493	850.81	0.038	309.997	31.096	763.08	0.041
284.997	31.262	857.79	0.037	314.988	35.187	770.89	0.040
290.000	36.082	864.96	0.037	320.001	39.230	778.16	0.039
294.995	40.876	871.98	0.037	325.007	43.268	785.31	0.039
299.996	45.676	878.94	0.036	329.999	47.271	792.22	0.038
304.995	50.437	885.68	0.036	335.001	51.260	798.91	0.038
309.998	55.170	892.23	0.036	340.005	55.193	805.27	0.037
314.992	59.868	898.61	0.035	345.011	59.105	811.46	0.037
320.001	64.536	904.78	0.035	279.991	2.214	673.07	0.056
259.980	2.063	784.52	0.044	284.993	6.137	682.93	0.053
264.989	6.657	792.10	0.043	289.996	10.076	692.53	0.050
269.986	11.387	800.62	0.041	294.992	14.009	701.79	0.048
274.991	16.234	809.71	0.040	299.993	17.948	710.76	0.046
279.996	20.972	817.93	0.040	304.993	21.878	719.43	0.045

https://doi.org/10.1021/acs.jced.2c00441
J. Chem. Eng. Data XXXX, XXX, XXX−XXX

Table 2. continued

T/K	p/MPa	c/m·s^{-1}	100·$U_c(c)/c$
309.996	25.790	727.73	0.044
314.991	29.685	735.75	0.043
319.998	33.553	743.39	0.042
325.006	37.412	750.83	0.041
329.999	41.287	758.23	0.040
335.001	45.049	764.91	0.039
340.005	48.821	771.52	0.039
345.011	52.604	778.11	0.038
284.993	2.110	642.52	0.061
289.995	5.821	652.71	0.057
294.991	9.556	662.70	0.054
299.992	13.287	672.24	0.051
304.993	17.012	681.38	0.049
309.995	20.732	690.18	0.047
314.991	24.443	698.68	0.046
320.000	28.154	706.90	0.045
325.005	31.837	714.75	0.043
329.997	35.487	722.25	0.042
335.001	39.122	729.47	0.041
340.006	42.776	736.65	0.041
345.011	46.456	743.90	0.040
289.994	2.192	613.06	0.068
294.990	5.706	623.66	0.063
299.992	9.233	633.86	0.058
304.992	12.766	643.65	0.055
309.995	16.303	653.07	0.053
314.989	19.772	661.69	0.051
320.000	23.259	670.05	0.049
325.005	26.752	678.25	0.047
329.997	30.229	686.17	0.045
335.001	33.685	693.71	0.044
340.005	37.135	701.05	0.043
345.011	40.576	708.20	0.042
294.989	2.296	583.37	0.076
299.991	5.649	594.73	0.069
304.991	8.996	605.32	0.064
309.993	12.342	615.53	0.060
314.989	15.684	625.15	0.057
319.999	19.030	634.35	0.054
325.005	22.363	643.14	0.051
329.997	25.677	651.53	0.049
335.001	28.969	659.45	0.048
340.005	32.258	667.15	0.046
345.010	35.550	674.71	0.045
299.991	2.399	552.48	0.087
304.990	5.541	564.15	0.078
309.994	8.689	575.38	0.071
314.989	11.756	584.83	0.066
319.999	14.912	594.89	0.062
325.004	18.065	604.37	0.058
329.996	21.195	613.32	0.056
334.999	24.317	621.80	0.053
340.005	27.433	629.98	0.051
345.011	30.545	637.89	0.049
304.989	2.572	521.79	0.101
309.993	5.521	534.24	0.089
314.987	8.473	545.55	0.080
319.998	11.428	556.19	0.073
325.005	14.385	566.27	0.068
329.996	17.334	575.82	0.064
335.000	20.267	584.74	0.060
340.005	23.195	593.28	0.057
345.011	26.130	601.58	0.055
309.991	2.748	489.85	0.120
314.988	5.494	502.72	0.104
319.997	8.261	514.68	0.092
325.003	11.026	525.74	0.083
329.996	13.790	535.75	0.076
335.001	16.540	545.58	0.071
340.005	19.295	554.64	0.066
345.011	22.053	563.75	0.063
314.987	2.916	455.52	0.148
319.997	5.468	469.10	0.125
325.004	8.027	482.06	0.109
329.996	10.590	493.29	0.097
334.999	13.149	504.24	0.087
340.006	15.711	513.74	0.080
345.011	18.282	523.64	0.074
319.997	3.628	432.62	0.169
325.002	6.014	445.99	0.141
329.995	8.407	458.70	0.122
335.000	10.811	470.14	0.107
340.005	13.218	480.73	0.097
345.011	15.631	490.88	0.088
334.999	8.201	424.23	0.149
340.006	10.398	436.18	0.130
345.011	12.603	446.13	0.115

[a]Speed of sound, c, values listed are averaged from up to 12 measurements at each state point. The relative combined expanded (k = 2) uncertainty of the speed of sound values, U_c (c). Only an average value for each (T, p) state point is given; see the Supporting Information for unaveraged data. The lines in the table separate the isochores. [b]The standard uncertainties for temperature and pressure are $u_c(T)$ = 0.004 K and $u_c(p)$ = 0.007 MPa, respectively.

observed for the present measurements or for those reported in our previous studies for mixtures of hydrofluorocarbons and hydrofluoroolefins.[33,35,37]

The crystal/spacer/reflector assembly was housed within a type 316 stainless-steel pressure vessel, which was, in turn, situated within a liquid bath whose temperature was measured using a standard platinum resistance thermometer (SPRT) located adjacent to the cell. The temperature control of the instrument was accomplished using the thermostated bath. A control program written in Visual Basic was used to confirm that the system achieved equilibrium before performing any measurements. Temperature and pressure information was logged by the program every 30 s, which was used to establish system equilibrium and stability from three criteria: (1) the difference of the average of the previous eight temperature scans from the setpoint, (2) the standard deviation of the previous eight temperature scans, and (3) the rate of pressure change with time calculated with a linear fit of the previous eight pressure readings. Once all three of these criteria were met within a preset tolerance, a converged flag was set in the control program, and the program entered a 30 min holding period to further establish the system's stability. While the temperature stability of the system was only observed in the bath (outside of the measuring cell), the pressure was a direct

Table 3. Experimental Vapor-Phase Density (p, ρ, T) Average Value Data for Difluoromethane, the Standard (k = 1) Uncertainty in Pressure, $u_c(p)$, the Relative Combined Expanded (k = 2) Uncertainty in Density, $U_c(\rho)$, and the Standard Uncertainty in Temperature, $u_c(T)$, of 3 mK[a]

T/K	p/MPa	ρ/kg·m^{-3}	$u_c(p)$/kPa	$100 \cdot U_c(\rho)/\rho$
240.003	0.10106	2.7165	0.030	0.124
240.001	0.12525	3.3914	0.030	0.090
240.000	0.14125	3.8434	0.030	0.081
240.000	0.16495	4.5216	0.030	0.069
240.000	0.18051	4.9732	0.030	0.064
239.999	0.20343	5.6466	0.030	0.057
249.997	0.10379	2.6680	0.030	0.113
250.000	0.12180	3.1447	0.030	0.094
250.000	0.14832	3.8554	0.030	0.077
250.001	0.16569	4.3264	0.030	0.069
250.001	0.18279	4.7946	0.030	0.063
250.001	0.20797	5.4921	0.030	0.055
250.001	0.22439	5.9527	0.030	0.052
250.001	0.23983	6.3895	0.030	0.048
250.001	0.26326	7.0606	0.031	0.045
250.001	0.28636	7.7314	0.031	0.040
250.001	0.30145	8.1748	0.031	0.039
259.998	0.12493	3.0897	0.030	0.098
260.001	0.16857	4.2085	0.030	0.071
260.002	0.20254	5.0949	0.030	0.058
260.002	0.24374	6.1895	0.030	0.049
260.002	0.28364	7.2711	0.031	0.042
260.002	0.32213	8.3355	0.031	0.037
260.001	0.36666	9.5943	0.031	0.033
260.002	0.40228	10.6233	0.031	0.031
260.002	0.44340	11.8375	0.031	0.028
260.002	0.48285	13.0306	0.032	0.026
269.999	0.15420	3.6782	0.030	0.085
270.001	0.21567	5.2044	0.030	0.061
270.002	0.25787	6.2746	0.030	0.050
270.002	0.30700	7.5442	0.031	0.041
270.002	0.35442	8.7951	0.031	0.036
270.002	0.39998	10.0223	0.031	0.032
270.002	0.45093	11.4253	0.031	0.030
270.002	0.50645	12.9944	0.032	0.025
270.002	0.55260	14.3320	0.032	0.024
270.002	0.60290	15.8270	0.032	0.022
270.002	0.65074	17.2876	0.033	0.020
280.000	0.20745	4.7945	0.030	0.062
280.002	0.26401	6.1595	0.031	0.049
280.002	0.31813	7.4916	0.031	0.041
280.002	0.37022	8.7988	0.031	0.035
280.002	0.42009	10.0743	0.031	0.032
280.002	0.46796	11.3223	0.032	0.028
280.002	0.51403	12.5458	0.032	0.026
280.002	0.55818	13.7407	0.032	0.024
280.002	0.60059	14.9097	0.032	0.023
280.001	0.68101	17.1869	0.033	0.020
280.002	0.71904	18.2933	0.033	0.019
280.002	0.75573	19.3802	0.034	0.019
280.002	0.82495	21.4857	0.034	0.017
280.002	0.85784	22.5130	0.035	0.017
280.002	0.92001	24.5052	0.035	0.016
290.000	0.24644	5.5064	0.030	0.055
290.001	0.36110	8.2069	0.031	0.039
290.002	0.41505	9.5117	0.031	0.034
290.001	0.51673	12.0346	0.032	0.027
290.002	0.56470	13.2555	0.032	0.025
290.002	0.65524	15.6175	0.033	0.022
290.002	0.73913	17.8779	0.034	0.020
290.002	0.81699	20.0435	0.034	0.018
290.002	0.89011	22.1409	0.035	0.017
290.002	0.99043	25.1295	0.036	0.016
290.001	1.05160	27.0206	0.037	0.015
290.002	1.13601	29.7250	0.038	0.014
290.002	1.21172	32.2543	0.039	0.013
299.998	0.24441	5.2546	0.030	0.061
300.001	0.39447	8.6475	0.031	0.038
300.001	0.55205	12.3660	0.033	0.029
300.001	0.62621	14.1763	0.033	0.024
300.001	0.77848	18.0260	0.034	0.020
300.001	0.84251	19.7026	0.034	0.018
300.001	0.96509	23.0173	0.036	0.016
300.001	1.12462	27.5610	0.038	0.015
300.001	1.21268	30.1942	0.039	0.014
300.001	1.32906	33.8298	0.040	0.013
300.001	1.46261	38.2503	0.042	0.012
300.002	1.56875	41.9830	0.042	0.012
300.001	1.65287	45.1025	0.045	0.011
310.001	0.30762	6.4219	0.031	0.046
310.001	0.48761	10.3952	0.032	0.032
310.001	0.64721	14.0692	0.033	0.024
310.001	0.78882	17.4606	0.034	0.020
310.001	0.91573	20.6155	0.035	0.018
310.002	1.06450	24.4671	0.037	0.017
310.001	1.19924	28.1138	0.039	0.015
310.002	1.37319	33.0736	0.041	0.013
310.001	1.51676	37.4118	0.043	0.013
310.001	1.51549	37.3764	0.153	0.020
310.001	1.66174	42.0571	0.154	0.019
319.993	0.20383	4.0638	0.030	0.075
319.995	0.32019	6.4582	0.031	0.048
319.995	0.73754	15.5472	0.034	0.022
319.995	0.73754	15.5475	0.034	0.022
319.995	0.73754	15.5476	0.034	0.022
319.995	0.73755	15.5477	0.034	0.022
319.995	0.92983	20.0360	0.037	0.021
319.999	0.19977	3.9814	0.030	0.072
319.999	0.32373	6.5319	0.031	0.045
319.999	0.43064	8.7843	0.031	0.035
319.998	0.54634	11.2802	0.032	0.028
319.999	0.64818	13.5302	0.033	0.024
319.998	0.74334	15.6797	0.034	0.022
319.999	0.84698	18.0762	0.035	0.021
319.999	0.92327	19.8789	0.036	0.018
319.999	1.00114	21.7545	0.036	0.017
319.999	1.19313	26.5435	0.039	0.015
319.999	1.26481	28.3966	0.039	0.015
319.999	1.31876	29.8162	0.041	0.014
319.999	1.40603	32.1600	0.042	0.014
319.998	1.51933	35.2959	0.044	0.013
319.998	1.60192	37.6535	0.045	0.013
339.994	0.20328	3.7993	0.030	0.077
339.994	0.33049	6.2392	0.031	0.047
339.994	0.44892	8.5559	0.031	0.039
339.995	0.52953	10.1592	0.032	0.032
339.995	0.62554	12.0970	0.033	0.027
339.995	0.71820	13.9981	0.033	0.024

https://doi.org/10.1021/acs.jced.2c00441
J. Chem. Eng. Data XXXX, XXX, XXX−XXX

Table 3. continued

T/K	p/MPa	ρ/kg·m^{-3}	$u_c(p)$/kPa	$100 \cdot U_c(\rho)/\rho$
339.995	0.81051	15.9229	0.034	0.022
339.995	1.02249	20.4671	0.037	0.018
339.995	1.08634	21.8719	0.037	0.018
339.994	1.23389	25.1842	0.040	0.017
339.994	1.33119	27.4228	0.042	0.016
339.994	1.43791	29.9296	0.043	0.015
339.994	1.51596	31.7987	0.044	0.015
339.994	1.61697	34.2655	0.045	0.014
290.005	0.23915	5.3357	0.030	0.058
290.003	0.32329	7.3035	0.031	0.042
290.003	0.40866	9.3538	0.031	0.034
290.003	0.48360	11.2007	0.032	0.028
290.003	0.56386	13.2317	0.032	0.025
290.003	0.64806	15.4250	0.033	0.022
290.003	0.72702	17.5447	0.034	0.020
290.003	0.80091	19.5880	0.034	0.018
290.003	0.88358	21.9484	0.035	0.017
290.003	0.96047	24.2200	0.036	0.016
290.003	1.04334	26.7593	0.037	0.015
290.004	1.12520	29.3693	0.038	0.014
290.003	1.20001	31.8531	0.039	0.013

[a]Data are presented in the sequence measured.

measurement of the fluid sample and, thus, stability of the pressure was an indication that the fluid sample was in thermal equilibrium with the surrounding bath fluid.

Prior to loading a sample, the system was evacuated to remove any residual sample from the previous test or solvent used to clean the system. Once the evacuation was complete, the bath temperature was set to its lower limit of 228 K and the sample was loaded. The speed of sound was measured along pseudo-isochores; measurements started at a pressure slightly greater than the bubble point curve at a temperature of 230 K, and up to 12 replicate speed of sound measurements were made at each (T, p) state point. Once measurements were complete at a given state point, the temperature was increased by an increment of 10 K, thus increasing the pressure. Measurements along pseudo-isochores were preferable over isotherms as they could be readily automated given the instrument's fixed-volume configuration. The procedure was repeated until the maximum temperature or pressure along the pseudo-isochore was reached; the temperature was then dropped to the starting point of the next isochore, and a portion of the sample was vented into a waste bottle to decrease the density.

2.3. Two-Sinker Densimeter. The two-sinker densimeter used to measure the (p−ρ−T) data is described in more detail elsewhere, and only key details are presented here.[38−40] This technique is based on the Archimedes principle used in a differential method and provides an absolute density measurement.[41] Two sinkers—one made of titanium and one of tantalum, with the same mass but different volumes—were immersed in the sample fluid and weighed, one at a time, via a magnetic suspension coupling. The basic working equation for the instrument gives the density

$$\rho_{\text{fluid}} = \frac{(m_1 - m_2) - (W_1 - W_2)}{V_1 - V_2} \tag{2}$$

where m_i are the sinker masses, W_i are the balance readings, V_i are the sinker volumes, and the subscripts refer to the two sinkers. Additional terms added to eq 2 compensate for the force-transmission error and also calibrate the balance.[39]

The temperature was determined using an SPRT located in a thermowell on the side of the measuring cell; it was calibrated on ITS-90 by using fixed-point cells in the temperature range from 83 to 505 K. Pressures were measured with one of two vibrating-quartz-crystal-type transducers having a full-scale pressure range of 2.75−14 MPa; these were calibrated by use of a piston gauge.

2.4. Measurement Uncertainty. For the pulse-echo instrument, the SPRT resistance was determined by ratio to a standard resistor using an AC resistance bridge; it was calibrated with five ITS90 fixed-point cells (mercury, water, indium, tin, and zinc). The combined standard temperature uncertainty included Type B contributions from the SPRT calibration and temperature gradients in the bath summing to 4 mK. Short-term variations in the bath temperature [calculated based on up to 12 replicates at each (T, p) state point] averaged 2 mK and were added as a Type A uncertainty for a total temperature standard uncertainty of 4 mK. The system pressure was measured using a vibrating quartz-crystal transducer with a standard uncertainty of 0.007 MPa and a full-scale range of 138 MPa; short-term variations in the pressure were also added as a Type A uncertainty. The combined expanded state-point uncertainty in the speed of sound measurements (i.e., also including the effects of temperature and pressure) was estimated by

$$\frac{U_c(c)}{\text{m}\cdot\text{s}^{-1}} = 2 \times \sqrt{\left\{u^2(c) + \left[\frac{\partial c}{\partial T}\right]^2 u^2(T) + \left[\frac{\partial c}{\partial p}\right]^2 u^2(p) + \left[\frac{\partial c}{\partial x_i}\right]^2 u^2(x_i)\right\}} \tag{3}$$

Major sources of uncertainty in the speed of sound were from the propane calibration of the path lengths[33,35] and the weaker echo signals as experiments approached the sample's critical point. The uncertainties in the temperature and pressure had a relatively small contribution to the combined uncertainty; variations between repeat determinations of the Δt [up to 12 replicates at each (T, p) state point] averaged 0.02%; details pertaining to the calculation of Δt are described elsewhere.[33] The uncertainty contribution from the composition was negligible since the samples used here had a purity of 99.99%. All speed of sound state point uncertainties reported in this study are calculated with a coverage factor, k = 2, or approximately 95% confidence level. Speed of sound relative combined expanded state point uncertainties are reported for each measurement since the uncertainties vary greatly with the magnitude of the speed of sound.

Experimental uncertainties for the two-sinker densimeter are discussed in detail in previous reports.[38,42] Details of the force transmission error analysis have also been previously reported.[39] The uncertainty in density with a coverage factor, k = 2, is given by

https://doi.org/10.1021/acs.jced.2c00441
J. Chem. Eng. Data XXXX, XXX, XXX−XXX

$$\frac{U_c(\rho)}{\mathrm{kg\cdot m^3}} = \left\{(52)^2 + \left[0.75\left(\frac{T}{K}\times 293\right)\right]^2 + \left(1.25\frac{p}{\mathrm{MPa}}\right)^2\right\}^{0.5}\frac{10^{-6}\rho}{\mathrm{kg\cdot m^3}} + 0.0014 \quad (4)$$

which accounts for the uncertainties in the weighings, sinker volumes, and force transmission error in the magnetic suspension coupling of the densimeter as well as corrections for vertical density gradients in the measuring cell. The standard uncertainty in the temperature is 3 mK. The standard uncertainty of the pressure measurement is $(40 \times 10^{-6}\cdot p + 0.06\ \mathrm{kPa})$ for the 2.75 MPa transducer and $(40 \times 10^{-6}\cdot p + 0.30\ \mathrm{kPa})$ for the 14 MPa transducer. In addition, the standard deviation of nine measurements of T and p made during the course of a density determination were added in quadrature as Type A uncertainties.

2.5. Validation of Dual-Path Pulse-Echo and Two-Sinker Densimeter Instruments. Unlike the two-sinker densimeter, the dual-path pulse-echo is a relative technique that requires calibration of the path-length difference before measurements. Calibration of the path-length difference in the pulse-echo instrument was performed with propane in November of 2019. This calibration was validated in December of 2021 immediately before experimental measurements for difluoromethane. Validation measurements were performed at temperatures ranging from 230 to 345 K up to pressures of 55 MPa. Figure 2 is a deviation graph comparing both the 2019 and 2021 propane data to the EOS of Lemmon et al.[43] Dashed lines represent the estimated uncertainty of the Lemmon et al. EOS, and error bars represent the relative combined expanded state point uncertainty for select 2021 propane speed of sound data points. The comparison of both data sets to the Lemmon et al. EOS is summarized using the absolute average deviation (Δ_{AAD}) and the maximum deviation (Δ_{MAX}) given by eqs 5 and 6, respectively,

$$\Delta_{\mathrm{AAD}} = 100\cdot\frac{1}{N}\sum_{i=0}^{N}\left|\frac{x_{i,\exp} - x_{i,\mathrm{EOS}}}{x_{i,\exp}}\right| \quad (5)$$

$$\Delta_{\mathrm{MAX}} = \max\left|\frac{x_{i,\exp} - x_{i,\mathrm{EOS}}}{x_{i,\exp}}\right| \quad (6)$$

where $x_{i,\exp}$ is an experimental data point, $x_{i,\mathrm{EOS}}$ is a value calculated using a reference EOS, and N is the number of data points. The Δ_{AAD} for both data sets in comparison to the Lemmon et al. EOS is 0.01% with Δ_{MAX} values of 0.11 and 0.06% for the 2021 and 2019 data sets, respectively.

The results in Figure 2 show that even after 2 years, the dual-path pulse-echo instrument calibration remained stable; during this time, measurements on 19 refrigerant mixtures were carried out.[33,35] Data tables containing the propane speed of sound data measured to validate the instrument are included in the Supporting Information.

The two-sinker densimeter is an absolute instrument, and thus, there is no calibration, per se. The performance of this instrument has been verified by comparison to *ab initio* calculations of the properties of helium[38] as well as comparisons to high-accuracy literature data on nitrogen[38]

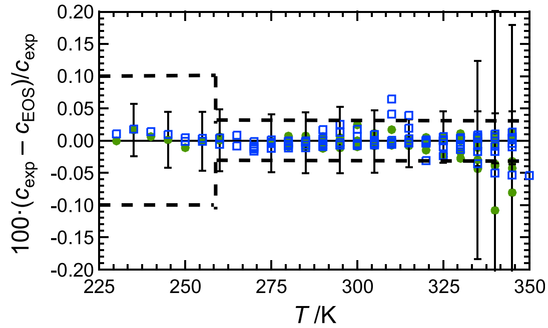

Figure 2. Comparison of measured propane speed of sound data, $c_{\exp}$, from 2021 (green circle solid) and 2019 (blue box) measurements to the Lemmon et al.[43] EOS, c_{EOS}. Dashed lines represent the estimated uncertainty of the EOS (0.1% $T < 260$ K and 0.03% 260 K $< T <$ 420 K). Error bars are the state point uncertainties of data points. Data were measured at pressures ranging from 1 to 52 MPa.

and propane. Validation of the performance over the full range of operating temperatures is described by McLinden.[44]

3. RESULTS

Reported in the following two sub-sections are the liquid-phase speed of sound data measured using a dual-path pulse-echo instrument and the vapor-phase density data measured using a two-sinker densimeter. Both instruments were custom-built and represent state-of-the-art measurement techniques resulting in low uncertainties for measured property values. Data sets are reported with relative combined expanded uncertainties.

3.1. Experimental Speed of Sound Data. The difluoromethane liquid-phase speed of sound was measured along isochores for a total of 209 (T, p, c) state points. Up to 12 replicates were measured at each (T, p) state point, and the averages are reported in Table 2; the combined expanded uncertainty of the averaged speed of sound measurements is also given. Unaveraged data and associated uncertainties are included in the Supporting Information.

3.2. Experimental Density Data. The difluoromethane vapor-phase density was measured along isotherms for a total of 138 (p, ρ, T) state points. Table 3 presents the pressure, temperature, and density averaged from up to five replicate measurements and the combined expanded uncertainty of the averaged measurements. The unaveraged data and their associated uncertainties are included in the Supporting Information.

4. DISCUSSION

Table 4 presents a summary of liquid-phase speed of sound and vapor-phase density measurements for difluoromethane considered by Tillner-Roth and Yokozeki in fitting their EOS[13] plus additional data published since 1997. Listed with the citations are the year of publication; the number of data points reported; purity of the difluoromethane sample used; temperature and pressure ranges of the data; reported uncertainties of the temperature, pressure, and speed of sound or density measurements; and absolute average and maximum deviations in comparison to the Tillner-Roth and Yokozeki EOS. It is important to reiterate that no literature studies specify the type of uncertainty (standard or expanded) reported. Uncertainties reported in this study are standard uncertainties in temperature and pressure and relative combined expanded uncertainties in vapor-phase density and speed of sound.

https://doi.org/10.1021/acs.jced.2c00441
J. Chem. Eng. Data XXXX, XXX, XXX−XXX

Table 4. Summary of Available Vapor-Phase Density Data and Liquid-Phase Speed of Sound Data for Difluoromethane[a]

source	year	N	purity (%)	range of data T/K	range of data p/MPa	uncertainties $u_c(T)$/mK	uncertainties $u_c(p)$/kPa	$100 \cdot U_c(y)/y$	Δ_{AAD}/%	Δ_{MAX}/%
Speed of Sound ($y = c$)										
this work	2022	210	99.99	230−340	2.1−70.0	4	14	0.035−0.17	0.37	0.75
Pires and Guedes[23]	1999	305	99.8	248−343	1.7−65.4	10	25	0.20	0.28	2.06
Grebenkov et al.[b,24]	1994	30		286−341	1.5−10.4	10	50	0.2 m s^{-1}[d]	0.18	0.51
Takagi[b,25]	1993	120		243−373	0.3−33.0	10	50	0.20	0.33	3.45
Vapor-Phase (p, ρ, T) Measurements ($y = \rho$)										
this work	2022	138	99.99	240−340	0.1−1.6	6	0.06−0.34	0.01−0.12	0.02	0.12
Bouchot and Richon[26]	1997	15	99.3	253−333	0.1−9.5	20	3	0.5 kg·m^{-3}[d]	2.01	6.25
deVries[b,27]	1995	94	99.99	243−373	0.07−5.7	5	0.02%[c]	0.03	0.05	2.87
Fukushima and Miki[45]	1995	158	99.98	314−424	1.9−10.1	10	3	0.20	1.08	7.18
Fu et al.[28]	1995	121	99.95	243−373	0.1−5.7	10	0.5	0.20	0.19	0.75
Defibaugh et al.[29]	1994	167	99.99	268−373	0.2−9.8	2	0.01	0.03	0.09	0.32
Sato et al.[30]	1994	69	99.998	330−410	4.2−9.4	7	0.4	0.20	0.25	4.23
Qian et al.[31]	1993	95	99.9	290−370	0.1−6.5	10	0.8	0.20	0.10	0.39
Malbrunot et al.[32]	1968	86	99.95	298−473	0.9−20.1	30	0.2	0.30	1.43	6.08

[a]Listed are the citations for each study; year published; number of data points reported; purity of the sample; ranges of temperatures (T) and pressures (p) studied; reported uncertainties of the temperature [$u_c(T)$], pressure [$u_c(p)$], and density or speed of sound measurements [$U_c(y)$]; and absolute average (Δ_{AAD}) and maximum deviations (Δ_{MAX}) in comparison to the Tillner-Roth and Yokozeki EOS.[13] [b]Denotes that these data were used in the development of the Tillner-Roth and Yokozeki EOS. [c]Authors reported a relative uncertainty rather than an absolute uncertainty. [d]Authors reported an absolute uncertainty rather than a relative uncertainty.

4.1. Comparison to Available Speed of Sound Data. Figures 3a and 3b compare the difluoromethane speed of sound data reported in this study and available literature data to values calculated using the Tillner-Roth and Yokozeki[13] EOS as a function of temperature and pressure, respectively.

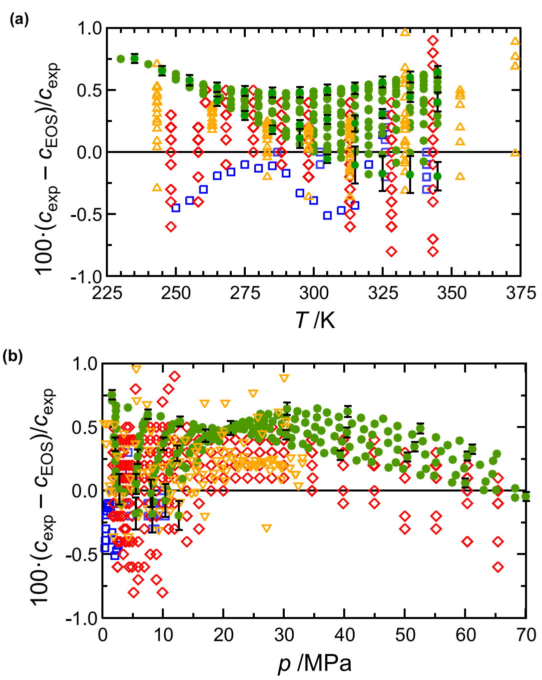

Figure 3. Comparison of the experimental speed of sound values, c_{exp}, to the calculated speed of sound values using the EOS of Tillner-Roth and Yokozeki,[13] c_{calc}, a function of (a) temperature and (b) pressure; green circle solid, this work; red diamond open, Pires and Guedes;[23] blue box, Grebenkov et al.;[24] and orange triangle down open, Takagi.[25] Error bars showing the relative combined expanded experimental uncertainty are shown for selected data obtained in this study.

All speed of sound data sets listed in Table 4 are included in the comparison. Error bars for select data reported in this study are included to illustrate the variation in the speed of sound state point uncertainty. The Δ_{AAD} for the present data is 0.37%, and this statistic ranges from 0.18 to 0.33% for the available literature data. The deviations are seen to vary systematically as a function of both temperature and pressure. The data reported in the present study agree with the available literature data, which were measured at frequencies ranging from 1 to 2.1 MHz, suggesting that no significant frequency dependence over a frequency range of at least 1−8 MHz occurs for the speed of sound of difluoromethane.

Tiller-Roth and Yokozeki do not state a speed of sound uncertainty for their EOS, although they estimate an uncertainty of 0.5−1% for the related quantity of isobaric heat capacity. In any event, these deviations in the speed of sound are substantially higher than the experimental uncertainty of the present measurements and other data sets reported in the literature. Tiller-Roth and Yokozeki stated that speed of sound was "fit with very low weight." They refer to speed of sound as "a sensible test for the accuracy of the derivatives" of the EOS. This is in contrast to recent EOS practice, where accurate speed of sound data are recognized as a vital element in the fitting.[46]

4.2. Comparison to Available Vapor-Phase Density Data. Figure 4 compares the vapor-phase density data from this work and those of de Vries[27] to vapor-phase densities calculated using the Tillner-Roth and Yokozeki[13] EOS. Included in Figure 4 are error bars representing the uncertainty for select data points and dashed lines drawn at ± 0.05% which Tillner-Roth and Yokozeki state is the "typical density uncertainty" of their EOS. The Δ_{AAD} is 0.02%, and all the data agree within the mutual uncertainties of the experiment and the EOS. Also shown in Figure 4 are deviations for the data of de Vries et al.;[27] these are the only vapor-phase density data used in fitting the EOS, and they are represented with an Δ_{AAD} of 0.05%. Although seven other vapor-phase (p, ρ, T) data sets, totaling 1276 data points, are available, they exhibit

https://doi.org/10.1021/acs.jced.2c00441
J. Chem. Eng. Data XXXX, XXX, XXX−XXX

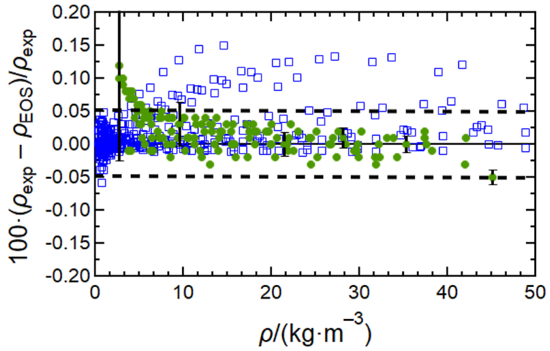

Figure 4. Deviation of experimental density values, ρ_{exp}, to density values calculated using the Helmholtz-energy-explicit EOS of Tillner-Roth and Yokozeki,[13] ρ_{EOS}, as a function of ρ_{exp}. Error bars represent the experimental uncertainty of select data points reported in the present study, and dashed lines at ±0.05% represent the "typical density uncertainty of 0.05%" reported by Tillner-Roth and Yokozeki; green circle solid, present study; blue box, de Vries.[27]

larger scatter and including them in Figure 4 would obscure the close agreement between the data reported in the present study and those measured by de Vries. These results indicate that the present EOS represents vapor-phase (p, ρ, T) behavior very well.

5. CONCLUSIONS

Difluoromethane is a material of interest in both the refrigerant and battery industries as the pursuit for sustainable next-generation technologies continues. Using custom, state-of-the-art instruments, this paper expands the liquid-phase speed of sound and vapor-phase density data available for difluoromethane. The relative expanded combined uncertainty (k = 2) in the speed of sound varied from 0.035 to 0.17% over a temperature range of 230−345 K, with pressures up to 70 MPa. These data deviate from the Tillner-Roth and Yokozeki[13] EOS by up to 0.79%, which is substantially higher than the experimental uncertainty for the speed of sound data presented in this paper. The uncertainty in vapor-phase densities ranged from 0.011 to 0.120% over a temperature range of 240−340 K, with pressures up to 1.61 MPa; these data are in good agreement with the Tillner-Roth and Yokozeki EOS, with an AAD of 0.02%. The data presented here are of high accuracy and will better characterize difluoromethane, which will aid in refitting efforts of a new EOS for difluoromethane. In turn, this will enable increased simulation accuracy, which can optimize next-generation sustainable technologies.

■ ASSOCIATED CONTENT

Supporting Information

The Supporting Information is available free of charge at https://pubs.acs.org/doi/10.1021/acs.jced.2c00441.

A description of the table headings for the files contained within the ZIP folder and averaged propane calibration data for the dual-path pulse-echo speed of sound instrument (PDF)

Difluoromethane data, unaveraged speed of sound experimental data (propane and difluoromethane), and unaveraged density experimental data (ZIP)

Liquid phase speed of sound and vapor phase density data can also be found at https://doi.org/10.18434/mds2-2554.

■ AUTHOR INFORMATION

Corresponding Author

Aaron J. Rowane − *Applied Chemicals and Materials Division, National Institute of Standards and Technology, Boulder, Colorado 80305, United States*; orcid.org/0000-0001-7605-0774; Email: Aaron.Rowane@nist.gov

Authors

Elizabeth G. Rasmussen − *Applied Chemicals and Materials Division, National Institute of Standards and Technology, Boulder, Colorado 80305, United States*; orcid.org/0000-0003-2871-6599

Mark O. McLinden − *Applied Chemicals and Materials Division, National Institute of Standards and Technology, Boulder, Colorado 80305, United States*; orcid.org/0000-0002-1082-309X

Complete contact information is available at: https://pubs.acs.org/10.1021/acs.jced.2c00441

Notes

The authors declare no competing financial interest.

■ ACKNOWLEDGMENTS

The authors would like to thank Stephanie Outcalt for her guidance in preparing the samples used for the speed of sound measurements and technical discussions pertaining to this work. The purity analysis of the pure fluids was provided by Thomas Bruno, Tara Lovestead, and Jason Widegren of the NIST. E.G.R. is currently a Research Associate Fellow of the National Research Council (NRC), which is overseen by the National Academies of Sciences, Engineering, and Medicine's (NASEM) Fellowships Office in partnership with the NIST (NIST-NRC).

■ REFERENCES

(1) BCC Research. *Refrigerants: Global Markets*; BCC Research: Wellesley, MA, USA, CHM159A, 2020; p 261.

(2) Coulomb, D.; Dupont, J.-L.; Morlet, V. *The Impact of the Refrigeration Sector on Climate Change-35. Informatory Note on Refrigeration Technologies*; IAEA, 2017.

(3) McLinden, M. O.; Seeton, C. J.; Pearson, A. New refrigerants and system configurations for vapor-compression refrigeration. *Science* **2020**, *370*, 791−796.

(4) Myhre, G.; Shindell, D.; Bréon, F.-M.; Collins, W.; Fuglestvedt, J.; Huang, J.; Koch, D.; Lamarque, J.; Lee, D.; Mendoza, B.; Nakajima, T.; Robock, A.; Stephens, G.; Takemura, T.; Zhang, H. Anthropogenic and Natural Radiative Forcing. *Climate Change 2013: The Physical Science Basis, Fifth Assessment Report of the Intergovernmental Panel on Climate Change*; Cambridge University Press: Cambridge, U.K., 2013.

(5) Environmental Protection Agency. Protection of Stratospheric Ozone. *Listing of Substitutes for Refrigeration and Air Conditioning and Revision of the Venting Prohibition for Certain Refrigerant Substitutes 80*; Environmental Protection Agency: Washington D.C, 2015; pp 19454−19501.

(6) Environmental Protection Agency. Protection of Stratospheric Ozone. *Listing of Substitutes under the Significant New Alternatives Policy Program; 86*; Environmental Protection Agency: Washington D.C, 2021; pp 24444−24474.

(7) ASHRAE. *ANSI/ASHRAE Standard 34-2019 Designation and Safety Classification of Refrigerants*; American Society of Heating, Refrigerating and Air-Conditioning Engineers: Atlanta, GA, 2019.

(8) Li, M.; Wang, C.; Chen, Z.; Xu, K.; Lu, J. New concepts in electrolytes. *Chem. Rev.* **2020**, *120*, 6783−6819.

(9) Ma, L.; Lee, J. Z.; Pollard, T. P.; Schroeder, M. A.; Limpert, M. A.; Craven, B.; Fess, S.; Rustomji, C. S.; Wang, C.; Borodin, O.; Xu, K. High-efficiency zinc-metal anode enabled by liquefied gas electrolytes. *ACS Energy Lett.* **2021**, *6*, 4426−4430.

(10) Yang, Y.; Davies, D. M.; Yin, Y.; Borodin, O.; Lee, J. Z.; Fang, C.; Olguin, M.; Zhang, Y.; Sablina, E. S.; Wang, X.; Rustomji, C. S.; Meng, Y. S. High-efficiency lithium-metal anode enabled by liquefied gas electrolytes. *Joule* **2019**, *3*, 1986−2000.

(11) Astina, I. M.; Sato, H. A rational Helmholtz fundamental equation of state for difluoromethane with an intermolecular potential background. *Int. J. Thermophys.* **2003**, *24*, 963−990.

(12) Outcalt, S.; McLinden, M. Equations of state for the thermodynamic properties of R32 (difluoromethane) and R125 (pentafluoroethane). *Int. J. Thermophys.* **1995**, *16*, 79−89.

(13) Tillner-Roth, R.; Yokozeki, A. An international standard equation of state for difluoromethane (R-32) for temperatures from the triple point at 136.34 K to 435 K and pressures up to 70 MPa. *J. Phys. Chem. Ref. Data* **1997**, *26*, 1273−1328.

(14) Lemmon, E.; Bell, I. H.; Huber, M.; McLinden, M. *NIST Standard Reference Database 23: Reference Fluid Thermodynamic and Transport Properties-REFPROP*, version 10.0; National Institute of Standards and Technology. Standard Reference Data Program: Gaithersburg, MD, 2018.

(15) Outcalt, S. L.; Rowane, A. J. Bubble point measurements of three binary mixtures of refrigerants: R-32/1234yf, R-32/1234ze(E), and R-1132a/1234yf. *J. Chem. Eng. Data* **2022**, *67*, 932−940.

(16) Outcalt, S. L.; Rowane, A. J. Bubble point measurements of mixtures of HFO and HFC refrigerants. *J. Chem. Eng. Data* **2021**, *66*, 4670−4683.

(17) Bell, I. H. Mixture models for refrigerants R-1234yf/134a, R-1234yf/1234ze (E), and R-134a/1234ze (E) and interim models for R-125/1234yf, R-1234ze (E)/227ea, and R-1234yf/152a. *J. Phys. Chem. Ref. Data* **2022**, *51*, 013103.

(18) Thol, M.; Lemmon, E. W. Equation of state for the thermodynamic properties of trans-1,3,3,3-tetrafluoropropene [R-1234ze(E)]. *Int. J. Thermophys.* **2016**, *37*, 28.

(19) Kazakov, A.; Muzny, C. D.; Kroenlein, K.; Diky, V.; Chirico, R. D.; Magee, J. W.; Abdulagatov, I. M.; Frenkel, M. NIST/TRC source data archival system: The next-generation data model for storage of thermophysical properties. *Int. J. Thermophys.* **2012**, *33*, 22−33.

(20) Chirico, R. D.; Frenkel, M.; Magee, J. W.; Diky, V.; Muzny, C. D.; Kazakov, A. F.; Kroenlein, K.; Abdulagatov, I.; Hardin, G. R.; Acree, W. E., Jr; Brenneke, J. F.; Brown, P. L.; Cummings, P. T.; de Loos, T. W.; Friend, D. G.; Goodwin, A. R. H.; Hansen, L. D.; Haynes, W. M.; Koga, N.; Mandelis, A.; Marsh, K. N.; Mathias, P. M.; McCabe, C.; O'Connell, J. P.; Pádua, A.; Rives, V.; Schick, C.; Trusler, J. P. M.; Vyazovkin, S.; Weir, R. D.; Wu, J. Improvement of quality in publication of experimental thermophysical property data: Challenges, assessment tools, global implementation, and online support. *J. Chem. Eng. Data* **2013**, *58*, 2699−2716.

(21) Diky, V.; O'Connell, J. P.; Abildskov, J.; Kroenlein, K.; Frenkel, M. Representation and validation of liquid densities for pure compounds and mixtures. *J. Chem. Eng. Data* **2015**, *60*, 3545−3553.

(22) Muzny, C. D. *NIST ThermoPlan—Experimental Planning and Coverage Evaluation Aid for Thermophysical Property Measurements*; National Institute of Standards and Technology: Boulder, Colorado, USA, 2013; Version *1*.

(23) Pires, P.; Guedes, H. The speed of sound and isentropic compressibility of liquid difluoromethane (HFC32) from T = (248 to 343) K and pressures up to 65 MPa. *J. Chem. Thermodyn.* **1999**, *31*, 55−69.

(24) Grebenkov, A. J.; Kotelevsky, Y. G.; Saplitza, V. V.; Beljaeva, O. V.; Zajatz, T. A.; Timofeev, B. D. Experimental study of thermal conductivity of some ozone safe refrigerants and speed of sound in their liquid phase, CFCs. *The Day after, Joint Meeting of IIR Commissions B1, B2, E1, and E2*; IIR: Padova, Italy, 1994; pp 419−429.

(25) Takagi, T. Ultrasonic speeds in liquid difluoromethane under high pressures. *High. Temp.—High. Press.* **1993**, *25*, 685−691.

(26) Bouchot, C.; Richon, D. Gas, liquid, and saturated vapor-liquid densities and vapor pressures of difluoromethane (R-32) and octafluoropropane (R-218) at temperatures from 253 K to 333 K and pressure up to 15.5 MPa. *Int. Electron. J. Phys.-Chem.* **1997**, *3*, 1−16.

(27) de Vries, B. *Thermodynamische Eigenschaften der alternativen Kältemittel R 32, R 125 und R 143a—Messungen und Zustandsgleichungen*; Universität Hannover, 1996.

(28) Fu, Y.-D.; Han, L.-Z.; Zhu, M.-S. PVT properties, vapor pressures and critical parameters of HFC-32. *Fluid Phase Equilib.* **1995**, *111*, 273−286.

(29) Defibaugh, D. R.; Morrison, G.; Weber, L. A. Thermodynamic properties of difluoromethane. *J. Chem. Eng. Data* **1994**, *39*, 333−340.

(30) Sato, T.; Sato, H.; Watanabe, K. PVT property measurements for difluoromethane. *J. Chem. Eng. Data* **1994**, *39*, 851−854.

(31) Qian, Z.-Y.; Nishimura, A.; Sato, H.; Watanabe, K. Compressibility factors and virial coefficients of difluoromethane (HFC-32) determined by Burnett method. *JSME Int. J., Ser. B* **1993**, *36*, 665−670.

(32) Malbrunot, P.; Meunier, P.; Scatena, G. M.; Mears, W. H.; Murphy, K. P.; Sinka, J. V. Pressure-volume-temperature behavior of difluoromethane. *J. Chem. Eng. Data* **1968**, *13*, 16−21.

(33) Rowane, A. J.; Perkins, R. A. Speed of sound measurements of binary mixtures of 1,1,1,2-tetrafluorethane, 2,3,3,3-tetrafluoropropene, and trans-1,3,3,3-tetrafluoropropene refrigerants. *J. Chem. Eng. Data* **2022**, *67*, 1365−1377.

(34) Bruno, T. J.; Fortin, T. J.; Huber, M. L.; Laesecke, A.; Lemmon, E. W.; Mansfield, E.; McLinden, M. O.; Outcalt, S. L.; Perkins, R. A.; Urness, K. N.; et al. *Thermophysical Properties of Polyol Ester Lubricants*; National Insititute of Standards and Technology: Gaithersburg, MD, 2019.

(35) Rowane, A. J.; Perkins, R. A. Speed of sound measurements of binary mixtures of difluoromethane (R-32) with 2, 3, 3, 3-tetrafluoropropene (R-1234yf) or trans-1, 3, 3, 3-tetrafluoropropene (R-1234ze (E)) refrigerants. *Int. J. Thermophys.* **2022**, *43*, 1−21.

(36) El Hawary, A.; Mirzaev, S. Z.; Meier, K. Speed-of-soun measurements in liquid n-pentane and isopentane. *J. Chem. Eng. Data* **2020**, *65*, 1243−1263.

(37) Rowane, A. J.; Perkins, R. A. Speed of sound measurements of binary mixtures of hydrofluorocarbons [pentafluoroethane (R-125), 1,1-difluoroethane (R-152a), or 1,1,1,2,3,3,3-heptafluoropropane (R-227ea)] with hydrofluoroolefins [2,3,3,3-tetrafluoropropene (R-1234yf) or trans-1,3,3,3-tetrafluoropropene (R-1234ze(E))]. *Int. J. Thermophys.* **2022**, *43*, 127.

(38) McLinden, M. O.; Lösch-Will, C. Apparatus for wide-ranging, high-accuracy fluid (p, ρ, T) measurements based on a compact two-sinker densimeter. *J. Chem. Thermodyn.* **2007**, *39*, 507−530.

(39) McLinden, M. O.; Kleinrahm, R.; Wagner, W. Force transmission errors in magnetic suspension densimeters. *Int. J. Thermophys.* **2007**, *28*, 429−448.

(40) Richter, M.; McLinden, M. O. Densimetry for the quantification of sorption phenomena on nonporous media near the dew point of fluid mixtures. *Sci. Rep.* **2017**, *7*, 1−13.

(41) Wagner, W.; Kleinrahm, R. Densimeters for very accurate density measurements of fluids over large ranges of temperature, pressure, and density. *Metrologia* **2004**, *41*, S24.

(42) McLinden, M. O.; Splett, J. D. A liquid density standard over wide ranges of temperature and pressure based on toluene. *J. Res. Natl. Inst. Stand. Technol.* **2008**, *113*, 29−67.

(43) Lemmon, E. W.; McLinden, M. O.; Wagner, W. Thermodynamic properties of propane III. A reference equation of state. *J. Chem. Eng. Data* **2009**, *54*, 3141−3180.

(44) McLinden, M. O. Densimetry for primary temperature metrology and a method for the in-situ determination of densimeter sinker volumes. *Meas. Sci. Technol.* **2006**, *17*, 2597−2612.

(45) Fukushima, M. O.; Miki, T. Thermodynamic properties measurements of HFC-32 and HFC-125. *Proceeding 19th International Congress of Refrigeration*; Institut international du froid: The Hague, The Netherlands, 1995; pp 207−214.

https://doi.org/10.1021/acs.jced.2c00441
J. Chem. Eng. Data XXXX, XXX, XXX−XXX

(46) Trusler, J. P. M.; Lemmon, E. W. Determination of the thermodynamic properties of water from the speed of sound. *J. Chem. Thermodyn.* **2016**, *109*, 61−70.

https://doi.org/10.1021/acs.jced.2c00441
J. Chem. Eng. Data XXXX, XXX, XXX−XXX